

Simulation and Modeling of an Energy Saving Electro-hydraulic Power Steering System of Vehicle

Robin Barua and Md. Mizanur Rahman

Institute of Energy Technology
Chittagong University of Engineering & Technology
Chattogram, Bangladesh
robi5374@gmail.com, mizanurr340@gmail.com

Md. Tazul Islam and Syed Masrur Ahmmad

Department of Mechanical Engineering
Chittagong University of Engineering & Technology
Chattogram, Bangladesh
tazul2003@cuet.ac.bd, masrur@cuet.ac.bd

Rasel Sen and Saswata Dutta

Department of Electrical and Electronic Engineering
Premier University
Chattogram, Bangladesh
rasel.sen.eee@gmail.com, saswata.an2@gmail.com

Abstract

The objective of this paper is to develop an energy saving model of power steering system of vehicle which can save energy and can provide driver a good steering feel according to vehicle speed and steering rate. The model is simulated in Matlab to show the energy consumption difference between existing and new model. The force developed in hydraulic actuator is proportional to motor speed. So, the speed of motor is controlled with pid controller to regulate the force. The speed of motor which is set point of pid controller changes according to steering rate and vehicle speed. The integral error at motor speed control at different speed is minimized using an adaptive integral gain lookup table with motor speed.

Keywords

Power steering, Motor speed map, Pid control, Energy and Steering effort.

1. Introduction

Steering system of a vehicle helps driver to control the direction of vehicle. Mechanical steering system uses driver's physical effort to steer vehicle's front wheels. But in power steering system, hydraulic force is used as an assist power for driver to move the front wheels with less physical effort. An engine driven vane pump continuously supplies fluid to develop assist power in hydraulic piston. A steering rotary valve operated by driver through steering column changes the direction of assist force according to desired direction. The driven power comes from vehicle engine. Conventional power steering system or hydraulic power steering system (HPS) consumes power at high speed which is a waste of fuel energy. As the world is now facing an energy crisis and carbon emission from transport is increasing day by day, electrification of this system can save the waste fuel and reduce emission. Normally in highway drive, 80% of the time steering angle remains less than 5°. At high speed, steering effort is lighter. So, hydraulic power generation greater than demand is a waste of energy in HPS. As open center rotary valve is used here, so if no steering occurs, there is always a circulation loss which is known as parasitic loss and this loss varies according to vehicle speed. This paper simulates an energy saving model of power steering system which uses an electric motor instead of vehicle engine to drive vane pump. Other hydraulic parts are same as conventional. By reducing the power delivery at high speed, this system saves energy. This system can be a solution

for electric power steering (EPS) in electric vehicles also where driver can't feel the road, as there is no hydraulic part. Efficient control of this system needed to increase driving comfort and make the system more energy efficient.

1.1 Objectives

The objective of this research is to develop a model of energy saving closed loop circuit which can save energy. Rack force is proportional to developed pressure at piston. And pressure is proportional to motor speed. So, the speed of motor is controlled by pid control algorithm. Motor speed is mapped according to vehicle speed and steering rate. Power consumption between energy saving power steering system and conventional power steering system is shown in Matlab simulation. The following outcomes can be achieved with this model:

- (i) Reduction of energy consumption.
- (ii) A good steering feel at different vehicle speed and obstacle avoidance at high speed.

2. Literature Review

Iga et al. (1987) developed the first motor driven power steering (MDPS) for Subaru XT in Japan, where a 12V motor is installed to drive the vane pump instead of vehicle engine. A controller decreases the motor speed to decrease power assist at high speed and provides natural steering sensation. The motor takes power from alternator which becomes a load of engine. But the test result shows that MDPS consumes low fuel as compared to conventional power steering. Gupta et al. (2018) developed an EHPS for medium duty truck FL 60 model. The gross weight of the vehicle is 23400 pound and front axle weight is 7900 pound. The result shows that the motor driven pump unit can supply maximum 5 lpm at 150 bar pressure, which is equivalent to 750 watt power, which is the working power of the system. As power is limited, so speed of steering is limited. Result shows that at low speed the conventional power steering is more energy efficient and at high speed EHPS is more efficient. Motor speed control is very important in EHPS system. Dong et al. (2018) designed a fuzzy-PID control strategy to control the speed of brushless dc motor. Motor speed has been increased than normal speed using field weakening method. The motor speed has been smoothly controlled under different load conditions. Motor speed control is the key of performance of EHPS system. Not only energy saving but also conventional HPS can give obstacle avoidance support at high speed. If vehicle travels at high speed and suddenly an obstacle come which needs to be avoided. Then higher flow rate supply develops higher pressure and rack speed gets higher. So, obstacle can be avoided. To available this rapid response at high speed in system, steering wheel angular velocity, motor speed and vehicle speed are the parameters have to be used (Chang-gao et al. 2011). Lin et al. (2014) simulated an induction motor control strategy for EHPS which can obtain good control effect. FUJITA(2001) developed a control method for brushless dc motor for Hydraulic-Electro power steering system to achieve steering feel and save energy. MURUGAN et al. (2008) developed electric power steering system which was implemented on light commercial vehicle. Brushless dc motor was used and torque was controlled to provide steering feel and motor had been directly connected to recirculating ball gear. For automobile with 42V dc supply, an electric driven pump unit was developed for EHPS system which was driven by an interior type synchronous motor (Rhyu et al. 2007). The hydraulic actuator of rack and pinion steering system used in light weight vehicles is a symmetrical actuator. Alaydi (2012) simulated and experimented a symmetrical actuator model where friction force and piston dynamic equations are included. Cologni (2016) also simulated an electro-hydraulic actuator model where special attention was given in friction model. Directional control valve or steering rotary valve is a major part of power steering system. Pressure developed in piston depends on valve structure also. Xu and Xu (2021) analyzed power steering valve where force, pressure and torque relation are discussed. Lu et al. (2012) have used fuzzy-adaptive PID control algorithm for motor speed control and calculated the power consumption at different vehicle speed. In EHPS system, for obstacle avoidance, high rack force is needed, so power consumption will be high. High power motor pump units, range from 500W-900W have been developed for low commercial vehicles (Gessat 2007). Positive displacement pump is used in EHPS system and the motor is controlled with pulse-width modulation signal. The differential pressure developed in the piston creates the actuating force to move front wheels (Kim and Kim 2012). The relationship between discharged flow rate and motor speed was tested by (Kim and Kim 2013).

3. System Description

The model shown in Figure 1 is similar to a conventional power steering system. But the modification is that, the vane pump is to be disconnected from vehicle engine and connected to a 12V dc brush motor with a belt. Fluid from vane pump comes to rotary valve through pressure tube. Rotary valve which is operated by driver via steering wheel and steering column changes the direction of fluid according to steering wheel direction. A microcontroller is to be used to take sensor input and to give signal output. Vehicle speed and steering rate sensor's value are the inputs of

the micro controller. And motor speed signal is the output of microcontroller. PID control algorithm runs in microcontroller CPU. The hydraulic piston rack moves right or left mechanically according to driver steering wheel direction. If steering wheel stays at neutral position, fluid returns to reservoir through return hose. If steering wheel is turned right or left, fluid goes to right or left piston respectively and develops pressure difference between chambers, to create actuating force. According to vehicle speed and steering rate value, motor speed control signal (PWM signal) is to be sent to motor drive circuit to control the motor speed, as well as to regulate the pressure difference which is linear to actuating force. PWM signal technique is energy efficient control method.

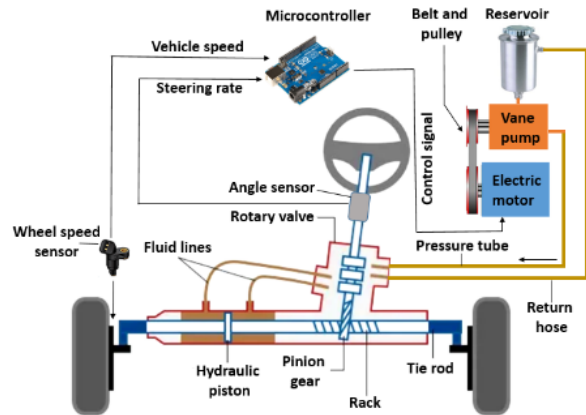


Figure 1. Energy saving power steering system

4. Modeling

4.1 Hydraulic power

The equation of power consumption of a load in hydraulic circuit is, multiplication of the pressure difference across the load and flow rate through the load (Daherand Ivantysynova2013).

$$\text{Power(W)} = \text{pressure(pa)} * \text{flow rate}\left(\frac{\text{m}^3}{\text{sec}}\right)$$

Unit conversion:

$$[\text{Watt}] = [\text{pascal} * \frac{\text{m}^3}{\text{sec}}] = [\frac{(\text{pascal} * \text{m}^2) * \text{m}}{\text{sec}}] = [\frac{\text{N} * \text{m}}{\text{s}}] = [\text{Watt}]$$

$$\begin{aligned} \text{Power(W)} &= \text{pressure(bar)} * 10^5 * \text{flow rate}\left(\frac{\text{litre}}{\text{min}}\right) * \left(\frac{1}{10^3 * 60}\right) = \frac{100}{60} * \text{pressure(bar)} * \text{flow rate}\left(\frac{\text{litre}}{\text{min}}\right) \\ &= \left[\frac{100}{60} * \text{pressure(bar)} * \text{flow rate}\left(\frac{\text{litre}}{\text{min}}\right)\right] \end{aligned}$$

$$\text{Power [kW]} = \frac{\text{pressure(bar)} * \text{flow rate}\left(\frac{\text{litre}}{\text{min}}\right)}{600}$$

The equation manufacturers' use for required input power to drive a pump is,

$$\text{Power [kW]} = \frac{p * Q}{600 * \text{efficiency}} \text{ (Kracht).}$$

4.2 Torque calculation

Power(W) = Torque(Nm) * angular velocity & Torque= Force*radius

$$P(W) = T(Nm) * 2\pi * \frac{\text{rotation}}{\text{sec}} = T(Nm) * 2\pi N, \text{ in Figure 2.}$$

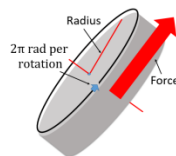


Figure 2. Force and torque relation

$$T(\text{Nm}) = \frac{P(W)}{2\pi N}$$

Manufacturer's equation to measure torque of a hydraulic pump(Kracht),

$$T(\text{Nm}) = \frac{P(\text{kW}) * 1000}{2\pi * \frac{N(\text{rpm})}{60}}$$

$$T = \frac{P(\text{kW})}{N(\text{rpm})} * \frac{60,000}{2\pi} = 9549 * \frac{P(\text{kW})}{N(\text{rpm})}$$

If we choose a 12V dc brush motor of 0.8 kilo-watt,

$$T = 9549 * \frac{0.8}{3000}$$

T=2.54 Nm rated motor will be needed to drive the vane pump.

4.3 Rack force calculation

Vehicle front axle weight, 500 kg, (Sindhu 2019)

Weight on each wheel=250 kg

Vertical force on each wheel=250*9.81 kg=2452.5 N

Steering force of each wheel= Vertical force*friction coefficient (μ) =2452.5*0.8=1962 N

Steering rack force to move both wheel= 1962*2=3924 N

4.4 Motor speed map according to friction coefficient, rack force and vehicle speed

Friction coefficient decreases with vehicle speed as shown in Figure 3 (a)(Cabrera 2018). The value of rack force in Figure 3 (b), is calculated by multiplying the vehicle vertical force (4900 N for 500kg) with friction coefficient at different vehicle speed. Steering force is linear with rack force and it is lesser than rack force because of using steering linkages and rack-pinion gear. So, rack force as well as steering force or driver steering effort decreases with vehicle speed. Here rack force is the force that is developed on vehicles tires due to vertical load, which is considered as, F_{load} . At different motor speed the developed piston force is calculated. The suitable motor speed will be the according to steering rate and driver's choice. And it needs practical implementation to determine the exact value. In sec 6, we have discussed in details.

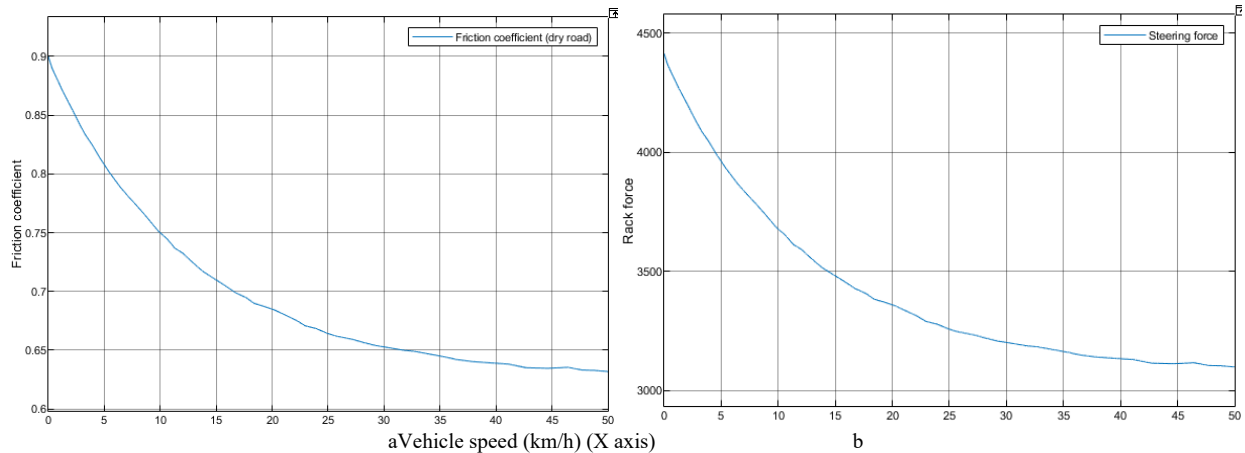


Figure 3.(a) Friction coefficient (dry road) versus vehicle longitudinal speed
(b) Rack force vs vehicle longitudinal speed

4.5 Pressure and force

If cylinder pressure develops 40 bar and piston cross sectional area=11.4cm² (used in simulation).

Then, 40 bar= 40*10⁵ Pascal=40*10⁵ Nm⁻² = (40*10⁵) / (100*100) Ncm⁻²=400 Ncm⁻²

Force on 1 cm²= 400N

Therefore, force on 11.4 cm²=400*11.4= 4560 N force can be developed with 40 bar pressure.

4.6 Hydraulic actuator model

The hydraulic actuator used in EHPS system is a symmetrical actuator. From the continuity of mass equation, we can find the pressure derivative (\dot{P}_a and \dot{P}_b) for each chamber (Academia). Q_{pump} is the supply flow rate of pump to chamber A. The equations, given below, show that pressure rate builds up linearly with flow rate (Q_{pump}). At neutral position of steering wheel, the piston stays at middle. So, both chambers volumes (V) are equal. And it changes as a function of piston position (x_p). Flow rate changes in chamber A and in chamber B as a function of piston velocity (\dot{x}_p). The equations are for piston rod moving left to right direction, as shown in Figure 4.

$$\dot{P}_a = \frac{\beta}{V + A_p x_p} (Q_{pump} - A_p \dot{x}_p)$$

$$\dot{P}_b = \frac{\beta}{V - A_p x_p} (A_p \dot{x}_p)$$

$$A_p = \pi * (B_r - R_r)^2$$

Where,

$$\dot{P}_a = \text{Derivative of pressure of chamber A, [pa]} \quad A_p = \text{Effective piston area, [m}^2\text{]}$$

$$\dot{P}_b = \text{Derivative of pressure of chamber B, [pa]} \quad B_r = \text{Cylinder bore radius, [m]}$$

$$\beta = \text{Bulk modulus, [N/m}^2\text{]} \quad R_r = \text{Rod radius, [m]}$$

$$V = \text{Fluid volume of half cylinder, [m}^3\text{]} \quad x_p = \text{Piston position, [m]}$$

$$Q_{pump} = \text{Pump flow rate, [m}^3\text{/s]} \quad \dot{x}_p = \text{Piston velocity, [ms}^{-1}\text{]}$$

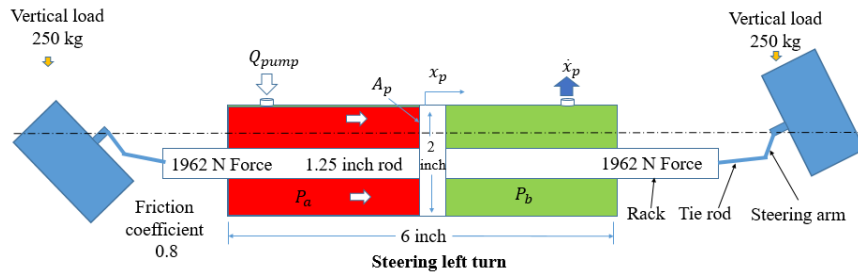


Figure 4. Hydraulic actuator model

After calculating the differential pressure of each chamber, we can know the total pressure developed in each chamber by integration. We can now calculate the acting force on piston by multiplying the effective piston area (A_p) with pressure difference across chambers. Here the equation,

$$F_p = A_p (P_a - P_b)$$

Where,

$$F_p = \text{Acting force on piston, [N]}$$

$$P_a = \text{Pressure of chamber A, [pa]}$$

$$P_b = \text{Pressure of chamber B, [pa]}$$

The piston motion equation can be developed from Newton's second law. As the piston force will move the tires, it is assumed that tire load F_{load} works as a linear spring load with a stiffness k . Friction force, F_{fric} between oil seal and piston also included which has components of viscous, coulomb and stibeck (seal) friction. The resulting force equation is,

$$F_p = m\ddot{x}_p + F_{fric} + F_{load}$$

$$F_{load} = kx_p$$

$$F_{fric} = F_{fric,v} + F_{fric,c} + F_{fric,s}$$

$$F_{fric,v} = k_v(\dot{x}_p)$$

$$F_{fric,c} = k_c \text{sign}(\dot{x}_p)$$

$$F_{fric,s} = k_s \text{sign}(\dot{x}_p) e^{-\frac{|\dot{x}_p|}{\tau_s}}$$

Where,

$$F_p = \text{Force developed on piston, [N]}$$

$$F_p = \text{Force developed on piston, [N]}$$

m =mass of piston and load, [kg]

\dot{x}_p =acceleration, [ms^{-2}]

F_{load} =Tire load, [N]

k = Tire stiffness,[Nm^{-1}]

F_{fric} =Summation of friction force, [N]

$F_{fric,v}$ =Viscous friction, [N]

$F_{fric,c}$ =Coulomb friction, [N]

$F_{fric,s}$ =Stribeck friction, [N]

k_v = Viscous friction coefficient (hydraulic viscosity), [kgs^{-1}]

τ_s = Stribeck velocity, [ms^{-1}]

F_{fric} has discontinuity in $\dot{x}_p = 0$, so $sign(\dot{x}_p)$ has been replaced by $\tanh(\dot{x}_p)$ and discontinuity has been removed (Cologni et al. 2016).

4.7 Vane pump flow

The vane pump of conventional HPS is a fixed displacement vane pump. The flow rate is proportional to the speed of vehicle engine speed. In this model, the vane pump will be driven by motor. For a single rotation, the displacement of vane pump is assumed $6 \text{ cm}^3 = 6 \cdot 10^{-6} \text{ m}^3$. Therefore the flow rate,

$$Q_{pump} = \frac{6 \cdot 10^{-6} \cdot \text{Motor rpm}}{60} (\text{m}^3 \cdot \text{s}^{-1})$$

5. Matlab Simulation

5.1 Motor speed control with PID

To simulate the motor speed control in Matlab, a dc brush motor's transfer function is used (Shamshiri 2009), where voltage is the input and angular rotation rate is the output. The speed of the dc brush motor is controlled via PID control method. The dc brush motor's transfer function is,

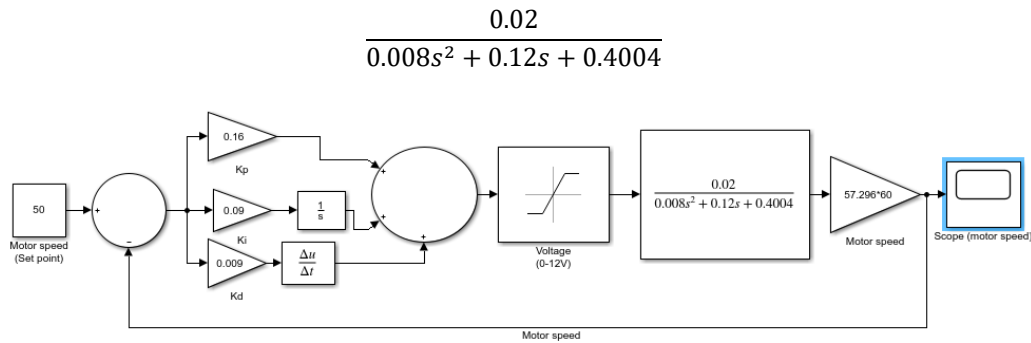


Figure 5. Motor speed control diagram

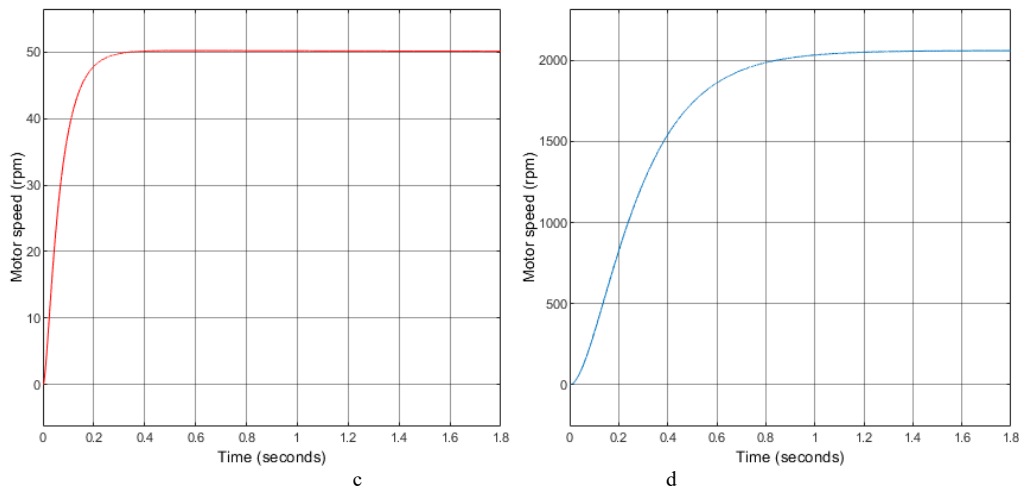


Figure 6. (c) Response curve for 50 rpm and

(d) 1500 rpm, for $K_p=0.16$, $K_i=0.09$, $K_d=0.01$

A 12 dc car battery (Li-ion) can be used as a power source, so the output of PID controller has been limited to 0-12 V. We give 12 V at transfer function input (open loop) and find motor speed is 2060 rpm. This the maximum motor speed. We will control the speed between 0-2000 rpm and it is suitable for vane pump. For closed loop, as shown in Figure 5 and Figure 6 (c), for motor speed 50 (set point), we have tuned the PID values as $K_p=0.16$, $K_i=0.09$ and $K_d=0.01$. But with increasing motor speed the overshoot is increasing for same PID values, for example 1500 rpm as shown in Figure 6 (d) and for different motor speed (set point) in Table 1. It's because of integral gain. For 500 motor speed, if we replace just the integral gain 0.09 with 0.060 then the overshoot is reduced. So, to minimize this overshoot for different motor speed set point, we have tuned the integral gain value only for different speed, Table 2. We have used a lookup table to set the suitable integral gain for different speed.

Table 1. Parameters of different motor speed set point

K _p =0.16, K _i =0.09, K _d =0.01									
Parameters	50 rpm	500 rpm	1000 rpm	1200 rpm	1500 rpm	1800 rpm	1850 rpm	1900 rpm	2000 rpm
Rise Time	0.1233	0.1335	0.1756	0.2041	0.2685	0.3654	0.3871	0.4115	0.4755
Settling Time	0.2221	0.2288	1.5884	2.0379	2.6633	3.3760	3.5471	3.8019	6.7093
Settling Min	45.0866	450.7500	901.9314	1.0824e+03	1.3524e+03	1.6220e+03	1.6671e+03	1.7113e+03	1.8075e+03
Settling Max	50.0437	507.4828	1.0364e+03	1.2557e+03	1.5956e+03	1.9528e+03	2.0111e+03	2.0545e+03	2.0606e+03
Overshoot	0.0870	1.4893	3.6251	4.6137	6.3376	8.4336	8.6508	8.0616	2.6468
Undershoot	0	0	0	0	0	0	0	0	0
Peak	50.0437	507.4828	1.0364e+03	1.2557e+03	1.5956e+03	1.9528e+03	2.0111e+03	2.0545e+03	2.0606e+03
Peak Time	0.5790	0.4640	0.4850	0.5110	0.5800	0.7990	0.9290	1.3120	6.2130

Table 2. Tuned Integral gain (K_i) for overshoot minimization at different speed

K _p =0.16, K _d =0.01									
Motor speed (rpm)	50	500	1000	1200	1500	1800	1850	1900	2000
Tuned Integral gain (K _i)	0.090	0.060	0.042	0.037	0.031	0.025	0.024	0.023	0.021
Overshoot	0.0870	0.0045	0.0466	0.0543	0.0836	0.0322	0.0204	0.0097	0.0013

5.2 Motor speed control with adaptive PID

Figure 6 shows the block diagram of updated integral gain for different speed which can be called adaptive PID control. Figure 7 (e) shows the lookup table output which is different integral gain at different speed. For a different motor speed set point (700 rpm) the simulation shows that, in Figure 7 (f), the adaptive PID has reduced the overshoot error.

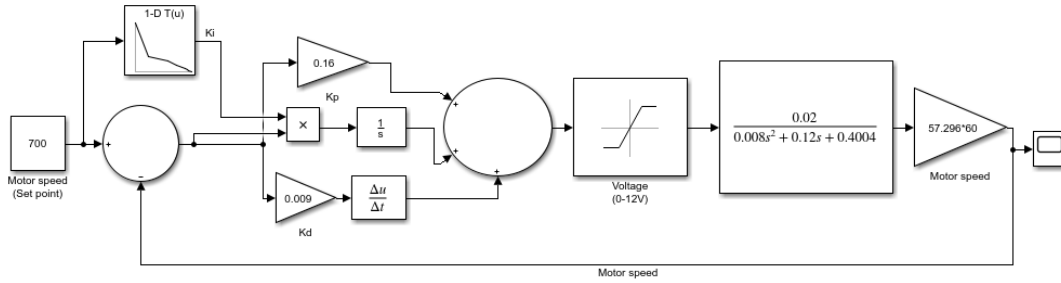


Figure 6. Motor speed control diagram with adaptive PID

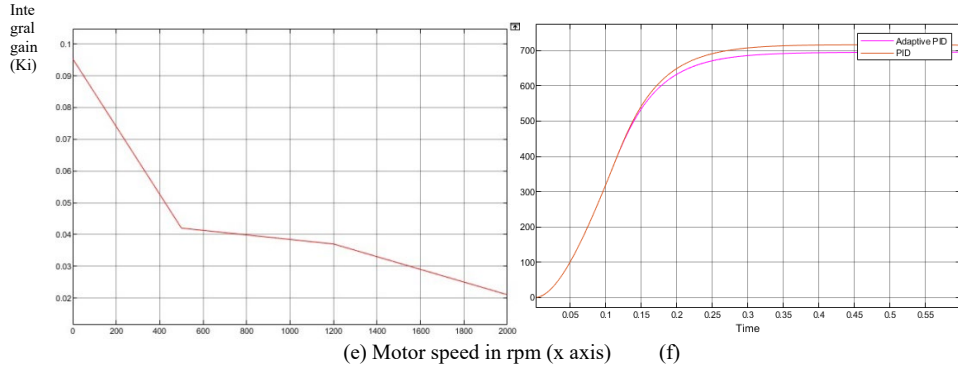


Figure 7. (e) Motor speed vs K_i , (f) Difference between adaptive PID and PID for set point 700 rpm

5.3 Hydraulic force control with varying speed

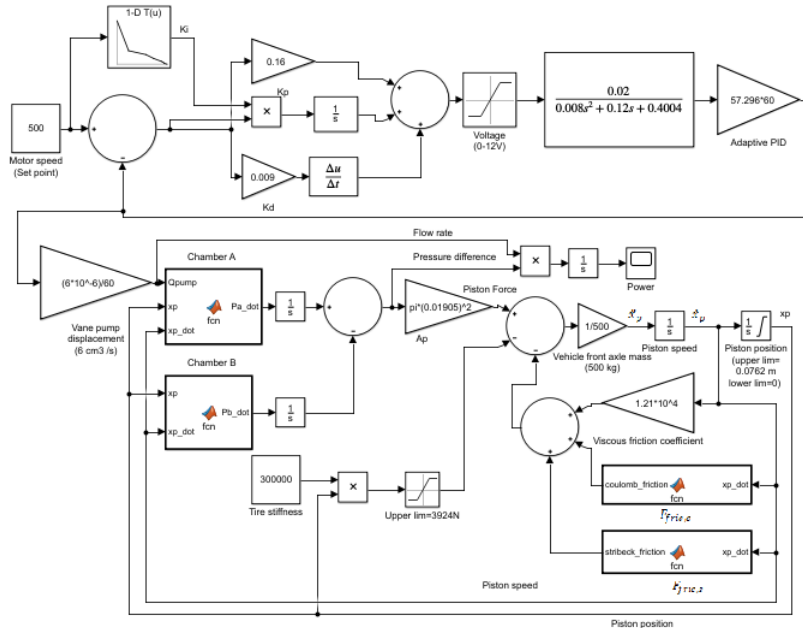


Figure 8. Hydraulic actuator block diagram

Table 4. Parameters for hydraulic actuator

Parameters	Value	Parameters	Value
β	$1.5 \times 10^9 \text{ Nm}^{-2}$	B_r	0.0508 m

x_p	0.0762 m	R_r	0.03175 m
A_p	$\pi \cdot 0.01905^2 \text{ m}^2$	k_v	$1.21 \cdot 10^4 \text{ kgs}^{-1}$
Q_{pump}	$\frac{6 \cdot 10^{-6} \cdot \text{Motor rpm}}{60} \text{ m}^3 \text{ s}^{-1}$	k_c	$1.14 \cdot 10^3 \text{ N}$
V	$\pi \cdot 0.01905^2 \cdot 0.0762 \text{ m}^3$	k_s	244.37 N
k	300000 Nm^{-1}	τ_s	$3.41 \cdot 10^{-3} \text{ ms}^{-1}$
m	500 kg		

6. Graphical Results

Steering feel at different speed and obstacle avoidance

Figure 9 shows piston force developed at different motor speed. The higher the motor speed the higher the piston force develops. If driver turns steering wheel fast it will provide fast assistance. If turns medium speed, the response will be medium.

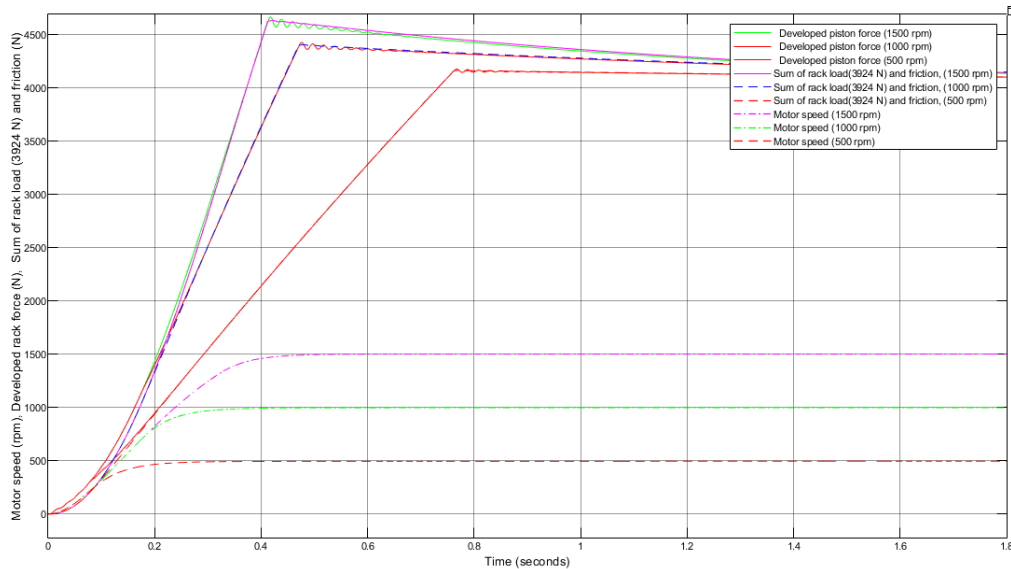


Figure 9. Developed piston force at different motor speed.

Low steering rate

If we look at Figure 3, when vehicle speed is approximately 6 kmph, the rack load is 3924 N at friction coefficient 0.8. And the total load is the summation of rack load (tire load) and friction load. If we set the motor speed set point 500 rpm. Then at 0.8 sec, Figure 9, the required piston force is developed which assists driver to steer wheel easily. And the rack displacement is 0.013m (0.51 inch) at 0.8 sec, Figure 11. The piston pressure is 36 bar (approximate) and flow rate is 2.5 liter per minute (lpm), Figure 12.

Medium steering rate

If driver needs quick steering, then microcontroller can detect it via steering rate sensor and will change the motor set point to 1000, for example. Then again from Figure 9, we can see that, the required rack force develops in 0.47 sec and rack displacement is 0.013m (0.51 inch) in 0.47 sec. The piston pressure is 38 bar (approximate) and flow rate is 6 lpm, Figure 12.

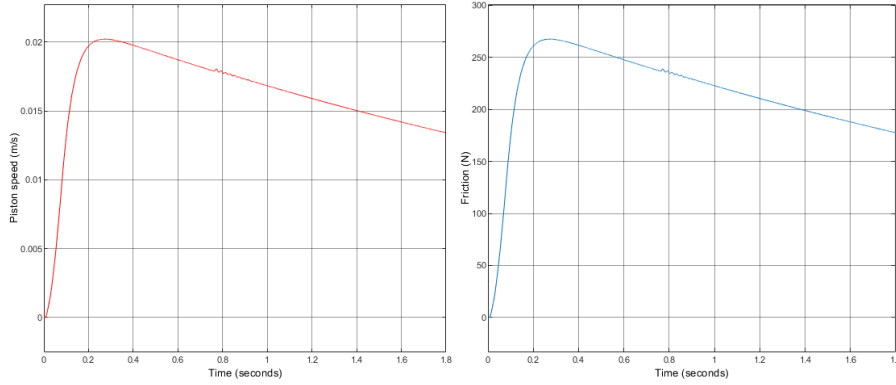


Figure 10. Friction and piston velocity

High steering rate

For high steering rate, motor speed will be high. Same as for 1500 rpm, the rack force develops in 0.41 sec and rack displacement is 0.013m (0.51 inch) in 0.41 sec. The piston pressure is 40 bar (approximate) and flow rate is 9 lpm. Figure 10 shows the relation between friction force and piston speed. Friction force changes as a function of piston speed. As motor speed increases, piston speed also increases, Figure 10.

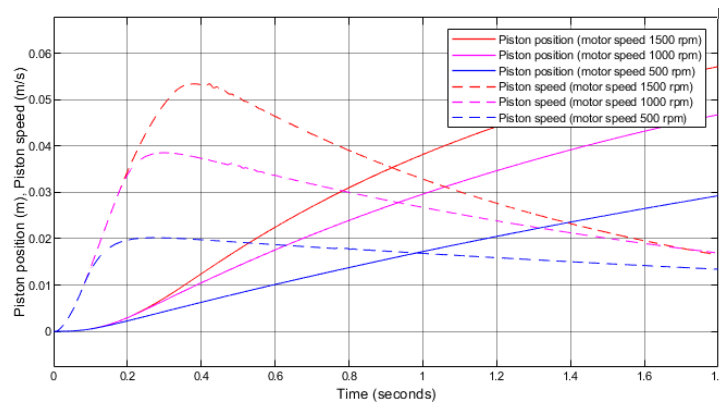


Figure 11. Piston position and piston velocity at different motor speed

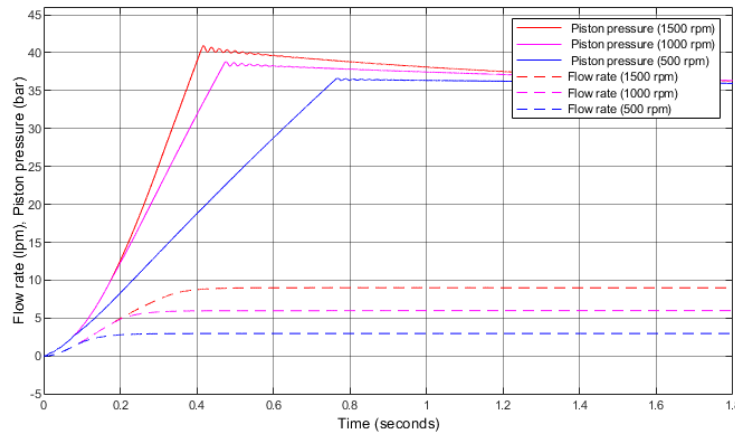


Figure 12. Vane pump supply and piston pressure at different motor speed

Energy consumption comparison

From Figure 13, we can see that at 500 rpm, at 1sec total energy consumption is 108 W. At 1000 rpm 272W and at 1500 rpm 422W. If we compare the old power steering system (engine driven HPS) with our model, we can see that the new model delivers fluid according to demand. Whereas engine driven HPS delivers fluid greater than demand at high speed.

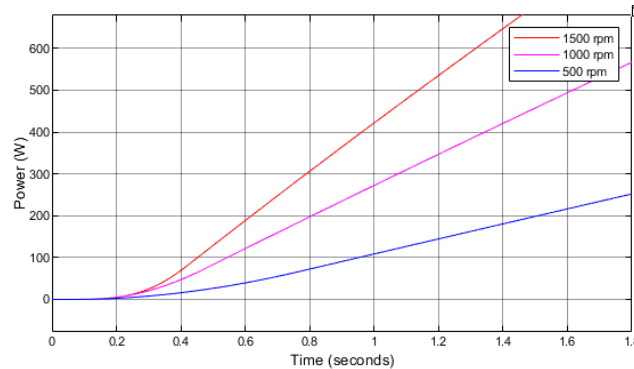


Figure 13. Power consumption at different motor speed

For example, from Figure 3(b) at 50 kmph rack force or tire load is 3100 N. In engine driven, the vane pump speed is as proportional to vehicle speed. The vane pump supplies fluid which develops piston force quick. But at high speed quick response not necessary unless for obstacle avoidance.

6. Conclusion

The result shows that the higher the motor speed the higher the flow rate increases. So the power consumption increases. In conventional power steering system the flow rate is low at low vehicle speed so the power consumption is low. But due to low flow rate the rack force is low. So it causes a hard steering feel to driver. At high vehicle speed, flow rate is high. But graph shows that, at high flow rate, the piston speed is high. But as friction coefficient decreases, so it causes very light steering feel. It's suitable for high speed obstacle avoidance. But not a good steering feel. On the other hand, in energy saving model, the flow rate is under control according to vehicle speed and steering rate. At low speed, it can provide maximum flow rate to reduce hard steering feel. And at high speed it can reduce flow rate as much as not needed. And at high speed, if steering rate is zero, then it can save energy by reducing the motor speed minimum. Which can be activated according to steering rate.

Acknowledgement

This paper is supported by Chittagong University of Engineering and Technology.

References

- Academia, Available: https://www.academia.edu/7629981/Actuator_Hydraulic_Equations
- Alaydi, J.Y., Modeling and Simulation of High-Performance Symmetrical Linear Actuator, *International Journal of Scientific & Engineering Research*, vol.3, no. 8, August 2012.
- Cabrera, J.A., Castillo, J.J., Perez, J., Velasco, J.M., Guerra, A.J., A procedure for Determining Tire-Road Friction Characteristics Using a Modification of the Magic Formula Based on Experimental Results, *Sensors* 2018, 18,896; doi:s18030896, 2018.
- Chang-gao, X., Zhong-ming, Z. and Rong-liang, Z., Realization of Control Algorithm for Electro-Hydraulic Power Steering System Based on MC9S08AW32, *International Conference on ICCE2011*, AISC 110, pp. 581-589, 2011.
- Cogni, A. L., Mazzoleni, M., Previdi, F., Modeling and Identification of an Electro-Hydraulic Actuator, *12th IEEE International Conference on Control & Automation (ICCA)*, Kathmandu, Nepal, June 1-3, 2016.
- Cogni, A.L., Mazzoleni, M., Previdi, F., Modeling and Identification of an Electro-Hydraulic Actuator, *12th IEEE International Conference on Control & Automation (ICCA)*, Kathmandu, Nepal, June 1-3, 2016.
- Daher, N. and Ivantysynova, M., Energy analysis of an original steering technology that saves fuel and boosts efficiency, *Energy Conversion and Management*, vol. 86, pp. 1059-1068, 2013.

- Dong, W., Song, J., Cheng, S., Yu, L. and Lu, X., Speed Control of BLDC Motor in Electro-Hydraulic Power Steering System Based on Fuzzy-PI Controller, *SAE Technical Paper 2018-01-0698*, 2018.
- Forbes, J. E., Baird, Steven M. and Weisgerber, T.W., Electrohydraulic Power steering – An Advanced System for Unique Applications, *International Congress and Exposition Detroit, Michigan, SAE Technical Paper Series 870574*, 1987.
- FUJITA, K., Development of Control Methods for Hydraulic-Electric Power Steering System Using Brushless DC Motor, *KOYO Engineering Journal English Edition No. 159E (2001)*.
- Gessat, J., Electrically Powered Hydraulic Steering Systems for Light Commercial Vehicles, *SAE TECHNICAL PAPER SERIES, 2007-01-4197*.
- Gupta, V., Williams, D. and Sherwin, K., Electrically Powered Hydraulic Steering on Medium duty Trucks, *SAE Int. J. Commer. Veh.* vol. 3, no. 1, 2011.
- Iga, S., Sakazaki, A. and Shibata, N., Motor Driven Power Steering- For the Maximum Steering Sensation in Every Driving Situation, *International Congress and Exposition, Detroit, Michigan, SAE Technical Paper Series 880705*, 1988.
- Kim, J., Kim, S., The Flow Rate Characteristics of External Gear Pump for EHPS, *4th International Conference on Intelligent Systems, Modelling and Simulation, 2013*.
- Kim, J., Kim, S., A Study on the Modeling and Analysis of an Electro-Hydraulic Power Steering System, *International Journal of Mechanical and Mechatronics Engineering*, vol. 6, no. 2, 2012.
- Kracht corp., High pressure gear pumps KP, <http://www.krachtcorp.com/mobile-hydraulics/high-pressure-gear-pumps-kp/>
- Lin, Li., Wang, W., Castillo, Liu, Zheng-qi., Modeling and Simulation of Slip Frequency Control for Induction motor in Electric Vehicle EHPS System, *Applied Mechanics and Materials*, vols.635-637, pp 1251-1255, 2014.
- Lu, W., Niu, G., Chen, L., Wang, R., Study on the Electro-hydraulic Power Steering System Based on AMESim and Simulink, *Advanced Materials Research*, vol. 422, pp 610-613, 2012.
- Ma, B., Yang, Y., Liu, Y., Ji, X., Zheng, H., Analysis of vehicle
- MURUGAN, R., NANDAKUMAR, S., MOHIYADEEN, M S., DSP-based electric power assisted steering using BLDC motor, *Sadhana*, vol.33, Part 5, October 2008, pp. 581-590, 2018.
- Rhyu, S., Kim, Y., Choi, J., Development of an Electric Driven Pump Unit for Electro-Hydraulic Power Steering of 42V Automobile, *0-7803-9761-4/07/\$20.00 IEEE, 2017*.
- Shamshiri, R.R., A Lecture Note on DC Motor Speed Control, Available: https://www.academia.edu/36416803/DC_Motor_Speed_Control, 2009.
- Sindhu R., Steering force calculation, Available: <https://skill-lync.com/student-projects/Steering-force-calculation-09215>, May 11, 2019.
- Xu, J., Xu, Y., Power steering control valve structural design optimization, *MEMAT 2021, Journal of Physics: Conference Series, 2021*.

Biographies

Robin Barua is pursuing an MSc in Energy Technology at Institute of Energy Technology, CUET, in the session of 2017-18. He received his BSc in EEE from Premier University, Chattogram, in 2017. After graduation, he served as an assistant project engineer for 6 months at Lucky Automation and Engineering Ltd. He has practical experience on installing fire detection and protection system. Also he has done some microcontroller and transistor based projects. His research interest includes electro-hydraulic system, motor control, automobile, energy saving techniques and fuzzy-pid control.

Dr. MdTazul Islam is a Professor of Department of Mechanical Engineering, CUET. He received his BSc, MSc and PhD in Mechanical Engineering from Bangladesh University of Engineering and Technology (BUET). His field of interest includes fluid mechanics and machinery, renewable energy and refrigeration, air conditioning and fuzzy-pid control. He has expertise in Hydrodynamics, Experimental Fluid Mechanics and Aerodynamics.

Syed Masrur Ahmmad is an Associate Professor of Department of Mechanical Engineering, CUET. He received his BSc in Mechanical Engineering from CUET and MSc in Mechatronics Engineering from International Islamic University Malaysia (IIUM). His field of interest includes mechatronics (control and robotics), applied mechanics. He has expertise in design engineering.

Md.Mizanur Rahman is pursuing an MSc in Energy Technology from CUET, in the session of 2017-2018. He received his BSc in Electrical and Electronic Engineering from the University of Information Technology and Science (UITS), Bangladesh in 2015. His research interest includes Energy Saving Techniques, Temperature Control, AI Techniques, Internet of Things , Electro- hydraulic system, Automobile, Fuzzy logic and PID control system.

Rasel Sen received his BSc in EEE from Premier University, Chattogram, in 2017. After graduation, he served as an assistant project engineer for 1 year at Lucky Automation and Engineering Ltd. He has practical experience on installing fire detection and protection system. His research interest includes ac motor, power system and smart grid system.

Saswata Dutta received his BSc in EEE from Premier University, Chattogram, in 2017. After graduation, he served as an assistant project engineer for 1 year at Lucky Automation and Engineering Ltd. He has practical experience on installing fire detection and protection system. His research interest includes pneumatic and hydraulic system, motor control and automation.